# LUND UNIVERSITY

**Fluid Flow, Combustion and Efficiency With Early or Late Inlet Valve Closing**

Söderberg, Fredrik; Johansson, Bengt

[Link to publication](Link to publication)

# Fluid Flow, Combustion and Efficiency with Early or Late Inlet Valve Closing

**Fredrik Söderberg and Bengt Johansson**
Lund Institute of Technology

**GLOBAL MOBILITY** DATABASE

*All SAE papers, standards, and selected books are abstracted and indexed in the SAE Global Mobility Database.*

**Printed in USA**

# Fluid Flow, Combustion and Efficiency with Early or Late Inlet Valve Closing

Fredrik Söderberg and Bengt Johansson
Lund Institute of Technology

## ABSTRACT

This paper is a study of the effects of valve timing and how it influences the in-cylinder fluid flow, the combustion, and the efficiency of the engine. An engine load of 4.0 bar imep$_{net}$ was achieved by setting the inlet valve closing time early or late to enable unthrottled operation. Inlet valve deactivation was also used and asymmetrical valve timing, i.e. valve timing with the two inlet valves opening and closing at different times. The valve timing was altered by switching cam lobes between the experiments.

The results indicate a longer flame development period but a faster combustion with early inlet valve closing compared to the throttled case. For late inlet valve closing, a variation in the combustion duration results. As expected, the pumping mean effective pressure (PMEP) was greatly reduced with early and late inlet valve closing compared to the throttled case.

## INTRODUCTION

In a normal four stroke spark ignited engine, the engine load is usually controlled by throttling the air flow into the engine. By lowering the pressure during the inlet stroke, higher pumping losses result as described by the pressure volume area enclosed during the change exchange process, see Figs. 43-50.

New engine technologies makes it possible to control the engine load with reduced pumping losses, e.g. by using different valve strategies or by diluting the inlet charge with exhaust gas recirculation (EGR) or air (lean burn).

Ford's camless engine [1] utilizes an electronically controlled hydraulic valve train. This system is very flexible, and can be used for load control. This system can either use early inlet valve closing (EIVC) or late inlet valve closing (LIVC), or it can be used to deactivate one or more cylinders at part load. This allows the other cylinders to operate at higher loads for a pumping work reduction. Theobald et. al. [2] suggests an efficiency improvement up to 12% during part load using load control with variable valve actuation.

Other systems use lost motion valves. This can be achieved in various different ways as described in [3]. This system can improve fuel economy by up to 15%. This highlights the magnitude of the compromise that fixed valve timing has.

Late inlet valve closing has been tested with both symmetric and with asymmetric valve events. With a symmetric valve event, tumble is induced in the cylinder and with an asymmetric valve event, swirl is induced, see Figures 4-6. This has also been shown by Wilson et. al. [4], who performed measurements in a flow rig, whereas the measurements in this paper are performed on an operating engine.

This paper presents several different strategies: early inlet valve closing, late inlet valve closing, symmetric and asymmetric valve strategies, normal valve timing and throttling and lean burn.

## EXPERIMENTAL APPARATUS

ENGINE - The experiments were conducted on a single cylinder version of the Volvo chrysler 2.5 liter Volvo B5254 engine. It is a four valves per cylinder engine with the geometric properties given in Table 1. The engine is modified to use one of the cylinders for combustion and the other four cylinders were motored using the standard pistons to help balance the system. This renders a single cylinder engine with the frictional losses of a five cylinder engine. Because of this, indicated mean effective pressure (IMEP), and not brake mean effective pressure (BMEP), has been used to determine engine load.

*Table 1: Geometric properties of the engine.*

| Displaced volume | 487 cm³ |
|---|---|
| Bore | 83 mm |
| Stroke | 90 mm |
| Geometric compression ratio | 10.3:1 |

The engine is equipped with mountings for a pressure transducer, located in the side of the pent roof combustion chamber (Fig. 1). The arrangement reduces the compression ratio from 10.4 to 10.3, but is not considered to influence the in-cylinder flow in a significant way. The engine can also be equipped with a quartz window in the opposite side of the cylinder. The shape of the window holder allows for velocity measurements along the entire cross section of the cylinder.

VARIABLE VALVE TIMING - The engine had no means of changing valve timing during engine operation. Instead, different cam shafts were used. They were designed to simulate load control with variable valve timing. The main interest was focused on part load operation, specifically 4.0 bar IMEP,net and 1500 rpm. This corresponds to steady state cruising in a passenger car.
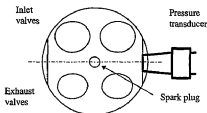


Figure 1: Arrangement for pressure measurements. This view is the cylinder head as seen from below.

In Figs. 2-6 the valve lift vs. crank angle is plotted together with the exhaust cam, the std cam (reference) and with the first part of the in-cylinder pressure. The valve strategies opening and closing times can be seen in Tables 2 and 3. The exhaust cam was left unchanged, (i.e. exhaust valve opening (EVO) 44° before bottom dead center (BBDC), exhaust valve closing (EVC) 16° after top dead center (ATDC), and a lift of 8.43 mm). The camshafts were designed to handle valve acceleration at 6000 rpm and the hertz contact pressure from the valve nose radius at low speeds.
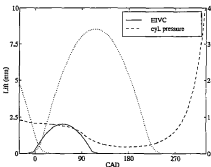


Fig. 2: Lift vs. crank angle for early inlet valve closing, 1.9 mm lift. The dotted lines are exhaust and reference cams.

THE PRESSURE MEASUREMENT SYSTEM - The pressure in the cylinder was measured with an AVL QC42 piezoelectric transducer connected to a Kistler 5001 charge amplifier. The charge amplifier voltage output was connected to a 486/33 PC with a Data Translation DT2823 100 kHz 16-bit A/D-card. A more detailed description can be found in [5].



Fig. 3: Lift vs. crank angle for late inlet valve closing, 9 mm lift. The dotted lines are exhaust and reference cams.



Fig. 4: Lift vs. crank angle for late inlet valve closing and asymmetric timing, 8.43 mm lift. The dotted lines are exhaust and reference cams.



Fig. 5: Lift vs. crank angle for late inlet valve closing and asymmetric timing, 3.6 mm lift. The dotted lines are exhaust and reference valves.
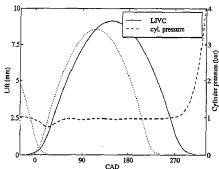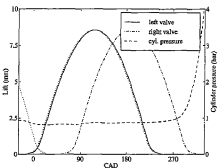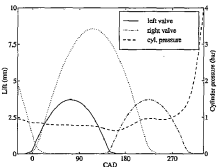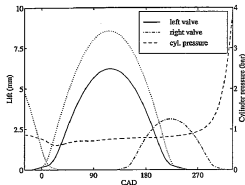
184

*Fig. 6: Lift vs. crank angle for late inlet valve closing and asymmetric timing, 6 and 3 mm lift. The dotted lines are exhaust and inlet cams.*

**LASER DOPPLER VELOCIMETRY SYSTEM** - A two component Laser Doppler Velocimetry (LDV) system from Dantec was used for the measurements. This system makes it possible to measure both horizontal and vertical velocity in each measurement point.

A cross section of the in-cylinder flow can be measured by traversing through the optical data. The optical data is processed by two Dantec Burst Spectrum Analyzers (BSA) connected to a PC. For a more thorough description, see Johansson et al.[5].

Laser Doppler Velocimetry requires particles called seeding to scatter the laser light. The seeding used was a polystyrene-latex dispersion, supplied with liquid atomizers. The resulting mean particle size is below one micron.

**SUPPLY SYSTEMS** - The engine was run on natural gas and gasoline. The natural gas was fed to the engine through a pulse width modulated solenoid valve upstream of the throttle and the gasoline was supplied via the standard port fuel injector. This is a single cone fuel injector. The contents of the natural gas used is given in Table 4. Unleaded gasoline with an octane number of 98 (RON) was used.

*Table 4: Contents of the natural gas used.*

| Component | Vol. % | Mass % |
|---|---|---|
| Methane | 91.1 | 81.0 |
| Ethane | 4.7 | 7.9 |
| Propane | 1.7 | 4.2 |
| n-Butane | 1.4 | 4.7 |
| Nitrogen | 0.6 | 0.9 |
| Carbon dioxide | 0.5 | 1.2 |

The solenoid valve and the fuel injector were controlled by a purpose built engine management system. When the engine was run on natural gas, the fuel was injected upstream of the throttle in the original five cylinder inlet manifold. The influence of different amounts of fuel and air into the engine from cycle-to-cycle was thereby reduced. The air/fuel-ratio was monitored by a Bosch LSM11 lean $\lambda$-sensor. The ignition power was supplied from a standard Transistorized Coil Ignition (TCI) system to a standard Volvo spark plug with production inlet penetration into the combustion chamber.

**THE CONTROL SYSTEM** - The ignition timing and skip-fire were controlled with a PC-based system. Triggering signals to the LDV and pressure systems were also included in this system. Input signals to the control system were a sync-pulse (1 pulse per 2 revolutions), a TDC-pulse (1 pulse per revolution) and a crank angle-pulse (5 pulses per crank angle degree, CAD).

*Table 2: Valve timing and lift for the symmetric valve timing cases. SDC represents the standard double cam. The prefix A and B represents after and before respectively, TDC means top dead center, and BDC bottom dead center. $p_i$ is the inlet manifold pressure.*

| Strategy | Open | Close | Lift (mm) | Duration | $p_i$ (kPa) |
|---|---|---|---|---|---|
| SDC | 8° BTDC | 232° ATDC | 8.43 | 240° | 43 |
| SDC, $\lambda$=1.5 | 8° BTDC | 232° ATDC | 8.43 | 240° | 56 |
| EIVC | 8° BTDC | 108° BBDC | 1.9 | 116° | 100 |
| LIVC 2x9 | 8° BBDC | 116° ABDC | 9.0 | 304° | 100 |

*Table 3: Valve timing and lift for the asymmetric valve timing cases. SSC represents the standard single cam. The prefix A and B represents after and before respectively, TDC means top dead center, and BDC bottom dead center. $p_i$ is the inlet manifold pressure.*

| Strategy | | Open | Close | Lift (mm) | Cam duration | Total duration | $p_i$ (kPa) |
|---|---|---|---|---|---|---|---|
| SSC | L | 8° ATDC | 232° ATDC | 8.43 | 240° | 240° | 43 |
| | R | - | - | - | - | | |
| SSC, $\lambda$=1.5 | L | 8° ATDC | 232° ATDC | 8.43 | 240° | 240° | 53 |
| | R | - | - | - | - | | |
| LIVC 1x9 | L | 8° BTDC | 296° ATDC | 9.0 | 304° | 304° | 100 |
| | R | - | - | - | - | | |
| LIVC | L | 8° BTDC | 232° ATDC | 8.43 | 240° | | 100 |
| | R | 50° ATDC | 296° ATDC | 8.43 | 240° | 304° | |
| LIVC | L | 8° BTDC | 144° ATDC | 3.6 | 152° | | 100 |
| | R | 146° ATDC | 296° ATDC | 3.6 | 152° | 304° | |
| LIVC | L | 8° BTDC | 162° ATDC | 6.0 | 170 | | 100 |
| | R | 146° ATDC | 296° ATDC | 3.0 | 150 | 304° | |

185

## OPERATING CONDITIONS

The engine speed was 1500 rpm and the engine load was 4 bar indicated mean effective pressure (IMEP, net). The results are reported at MBT ignition timing. The choice of IMEP instead of BMEP as a reference is due to the special design of the single cylinder engine which has the frictional losses of a five-cylinder. In addition, day-to-day frictional differences are eliminated. When the engine was operated with the standard cam shaft and throttle, two different air/fuel ratios were tested.

The engine was operated in a skip fire mode for the LDV measurements. This means that the ignition is turned off during the measurements. This mode of operation was necessary to ensure the required seeding particle density. During skip fire, the engine is fired ten cycles and then motored one cycle.

## DATA PROCESSING

VELOCITY PARAMETERS - For each component and cycle, the velocity trace was low-pass filtered with the moving window technique [6] to extract a "mean velocity". In the moving window procedure the mean value of the velocity samples within a specified crank angle window is considered to represent the mean velocity in the center of the window. To get a smoother low-pass filtering a Hanning window was also introduced. The "mean velocity" in a window was then obtained from

$$\overline{U}(\theta) = \frac{\sum_{\varphi(i)\theta-\alpha/2}^{\varphi(i)\theta+\alpha/2} U(i) \ 0.5 \left\{1 - \cos\left[2\pi\left(\frac{\varphi(i) - \theta + \alpha/2}{\alpha}\right)\right]\right\}}{\sum_{\varphi(i)\theta-\alpha/2}^{\varphi(i)\theta+\alpha/2} 0.5 \left\{1 - \cos\left[2\pi\left(\frac{\varphi(i) - \theta + \alpha/2}{\alpha}\right)\right]\right\}}$$

where

$\theta$ = Crank angle position where the mean velocity should be calculated.

$\alpha$ = Width of the crank angle window used in the lowpass filtering.

$\varphi(i)$ = Crank angle position of velocity registration $i$.

The turbulence is then calculated as the difference between the slowly changing mean velocity and instantaneous velocity registrations within a crank angle window according to

$$u(\theta) = \left(\frac{\sum_{\varphi(i)\theta-\alpha/2}^{\varphi(i)\theta+\alpha/2} u(i)^2}{\left(\sum_{\varphi(i)\theta-\alpha/2}^{\varphi(i)\theta+\alpha/2} i\right) - 1}\right)^{1/2} = \left(\frac{\sum_{\varphi(i)\theta-\alpha/2}^{\varphi(i)\theta+\alpha/2} [U(i) - \overline{U}(i)]^2}{\left(\sum_{\varphi(i)\theta-\alpha/2}^{\varphi(i)\theta+\alpha/2} i\right) - 1}\right)^{1/2}$$

where the mean velocity at the crank angle position $i$ is obtained with linear interpolation.

The moving window technique requires a cut-off frequency to be chosen. This cut-off frequency separates mean velocity transients during the engine cycle and turbulence. If a small window is used, there is a problem with accuracy due to limited data rate, and if the window is wide, the assumption must be made that the flow changes very slowly within the cycle. The average data rate was 40-70 kHz giving between 53 and 93 data points within a 12 degree window at 1500 rpm. If the assumption is made that the samples are independent, the resulting uncertainty in the RMS calculation can be estimated at 14%. The results presented are calculated with a window of 12 degrees corresponding to a cut-off frequency of 750 Hz.

For each measurement location 200-250 engine cycles were collected. The results presented are the average value of mean velocity and turbulence as well as the standard deviation from cycle to cycle.

ONE-ZONE HEAT RELEASE MODEL - To extract information on the flame development, a cycle-resolved heat release calculation was performed. In the computations Woschni's heat transfer model [7] was applied and the ratio of specific heats was assumed to have a linear dependence on temperature. Further details concerning the heat release calculation have been described elsewhere [8]. For each operating condition, 300 engine cycles were obtained to form the combustion parameters presented.

## FLOW RESULTS

The turbulence influences the flame speed, and it has been shown that turbulence gives fast combustion [5]. However, the mean velocity can make the combustion slower due to wall cooling of the flame or by quenching.

Flow results will be presented for the different valve timing strategies and a comparison between the different strategies will be presented for some of the strategies. Horizontal velocity, vertical velocity, and average turbulence will be presented.

STANDARD DOUBLE CAM, THROTTLED TO 4 BAR IMEP,NET - In this study, the standard double cam is used as the baseline configuration. The high double cam induces a tumble flow in the cylinder, which can be seen in Fig. 7. The horizontal velocity is lower at the side of the cylinder. The vertical velocity only reflects the piston movement, see Fig. 8. The turbulence is homogenous, and has a peak at 20 CAD BTDC, see in Figs. 9 and 31.

STANDARD SINGLE CAM, THROTTLED TO 4 BAR IMEP,NET - The standard single cam corresponds to valve deactivation. The horizontal velocity shows a clear swirling pattern. At TDC, the swirl disappears but after TDC it returns with slightly lower velocity, see Fig. 10. The vertical velocity shows signs of the piston movement, as above, but the velocity is inhomogeneous, see Fig. 11. The turbulence is higher with inlet valve deactivation, and is approximately 1.7 m/s at TDC, see Figures 12 and 31.

EARLY INLET VALVE CLOSING (EIVC), 1.9 MM LIFT - The low lift and the short open duration gave a low horizontal and vertical velocity, see Figures 13 and 14. The turbulence is

also very low (below one meter per second at TDC), see Figures 15 and 31.

LATE INLET VALVE CLOSING (LIVC), 1x9 MM LIFT - The valve strategy using late inlet valve closing and valve deactivation produces a swirl, see Figure 16. It is not as pronounced as for the standard single cam. The vertical velocity is very inhomogeneous and no clear trends can be seen, see Fig. 17. The turbulence is very high, approximately 2.6 m/s at TDC, see Figs. 18 and 31.

LATE INLET VALVE CLOSING (LIVC), 2x9 MM LIFT - Late inlet valve closing has a large open duration. This symmetric high lift and long duration gives a tumble flow that can be seen in Fig. 19. The horizontal velocity is approximately free meter per second. The vertical velocity reflects the piston movement, see Fig. 20. The turbulence is approximately 1 m/s at TDC, see Figs. 21 and 32.

LATE INLET VALVE CLOSING (LIVC) WITH ASYMMETRIC VALVES, 8.43 MM LIFT - The valve strategy with late inlet valve closing, high lift and asymmetric timing gives a complex flow pattern. There is a trace of swirl in the beginning but it is replaced by something resembling a double vortex at TDC. The flow changes after TDC, see Fig. 22. The vertical velocity shows the movement of the piston very clearly, see Fig. 23. The turbulence is approximately 1.5 m/s at TDC, see Figs. 24 and 32.

LATE INLET VALVE CLOSING (LIVC) WITH ASYMMETRIC VALVES, 3.6 MM LIFT - The strategy with late inlet valve closing, asymmetric timing and relatively low lift induces a tumble that disappears rapidly. At TDC the horizontal velocity is relatively low, see Fig. 25. The vertical velocity indicates a double vortex, but this pattern disappears after TDC, see Fig. 26. This valve strategy creates the strongest turbulence, 2.8 m/s, see Fig. 27 and 32.

LATE INLET VALVE CLOSING (LIVC) WITH ASYMMETRIC VALVES, 6 AND 3 MM LIFT - This valve strategy was designed to induce swirl in the engine, and this can be seen in Fig. 28. The swirl almost disappears at TDC, and is thereafter almost constant. The vertical velocity is very inhomogeneous and shows signs of a double vortex but this trend disappears after TDC, see Fig. 29. The turbulence is high, 2.7 m/s, see Fig. 30 and 32.

THE FLOW IN THE VICINITY OF THE SPARK PLUG - Figures 31-45 show the state of the flow in the vicinity (i.e. within three mm) of the spark plug. Figures 31-32 show the turbulence in the vicinity of the spark plug and Figures 33-34 show the standard deviation of turbulence in the vicinity of the spark plug. It can be seen that the standard deviation is high for LIVC 1x9 mm and the standard single cam, but this is due to the higher turbulence for those strategies. Late inlet valve closing with an asymmetric 3.6 mm lift and late inlet valve closing with an asymmetric 6+3 mm lift have the largest standard deviation. This mean that the coefficient of variation (COV) of the turbulence is roughly the same for all strategies.

Figure 35 shows the horizontal mean velocity in the vicinity of the spark plug. It can be seen that early inlet valve closing has

very low horizontal velocity, as seen before. Late inlet valve closing with valve deactivation has large negative horizontal velocity at 80 CAD BTDC, but stabilizes around zero at TDC. The standard double cam has approximately the same appearance from 30 CAD BTDC to 40 CAD ATDC. In Fig. 36, it can be seen that late inlet valve closing, 2x9 mm lift has approximately the same appearance as late inlet valve closing and valve deactivation (see Fig. 35). The other valve strategies in Fig. 36 show a similar behavior and late inlet valve closing with an asymmetric 3.6 mm lift has the greatest horizontal velocity, 12 m/s at 55 CAD BTDC.

In Fig. 37-38 the vertical velocity in the vicinity of the spark plug can be seen. The vertical piston motion can be seen in both figures, giving an upward flow before TDC and a downward flow after TDC. However, early inlet valve closing has a vertical velocity close to zero before TDC. In Fig. 38 it can be seen that the strategies all produce approximately the same vertical velocities. The only outlier is late inlet valve closing with an asymmetric 8.43 mm lift (std). It has a slightly higher vertical velocity during 40 CAD BTDC to 20 CAD BTDC and this will shape up in the results for the flame development period and the combustion rate.

Figures 39 and 40 show the standard deviation of mean velocity in the vicinity of the spark plug, for natural gas and gasoline. The standard deviation of mean velocity added to the turbulence gives the ensemble averaged turbulence. The plots of the turbulence and the plots for the standard deviation of mean velocity are very similar, see Figs. 31-32 and 39-40.

Figures 41 and 42 show the anisotropy of turbulence. This is a measure of the uniformity of the turbulence in the two measured directions. It can be seen that the turbulence is approximately isotropic from 20 CAD BTDC and during the combustion period. The highest anisotropy is created by late inlet valve closing and valve deactivation. In Fig. 42, it can be seen that late inlet valve closing with an asymmetric 6+3 mm lift, LIVC with an asymmetric 3.6 mm lift and LIVC with an asymmetric 8.43 mm (std) lift produce large anisotropy.
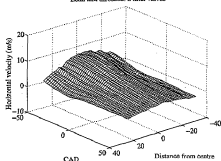
Fig. 7: Horizontal velocity for the standard double cam.
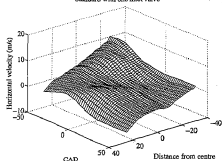


Fig. 10: Horizontal velocity for the standard single cam.
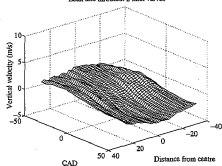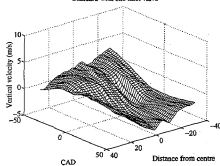


Fig. 8: Vertical velocity for the standard double cam. This is the reference cam.



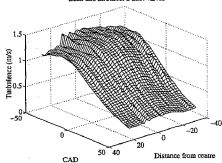Fig. 11: Vertical velocity for the standard single cam. This represents valve deactivation.



Fig. 9: Turbulence for the standard double cam.
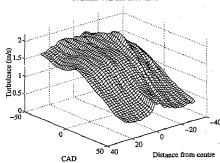


Fig. 12: Turbulence for the standard single cam.
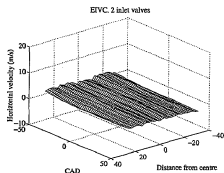
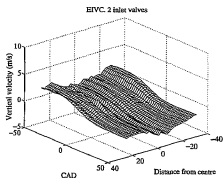*Fig. 13: Horizontal velocity for early inlet valve closing.*



*Fig. 16: Horizontal velocity for late inlet valve closing, 1x9 mm lift (valve deactivation).*



*Fig. 14: Vertical velocity for early inlet valve closing.*
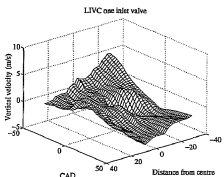


*Fig. 17: Vertical velocity for late inlet valve closing, 1x9 mm lift (valve deactivation).*



*Fig. 15: Turbulence for early inlet valve closing.*
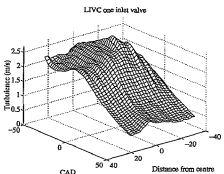


*Fig. 18: Turbulence for late inlet valve closing, 1x9 mm lift (valve deactivation).*

189
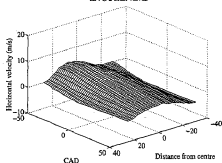
*Fig. 19: Horizontal velocity for late inlet valve closing, 2x9 mm lift.*
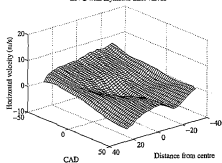


*Fig. 22: Horizontal velocity for asymmetric late inlet valve closing, 8.43 mm lift.*
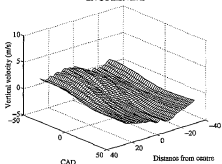


*Fig. 20: Vertical velocity for late inlet valve closing, 2x9 mm lift.*



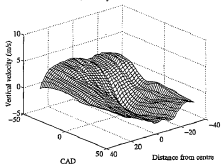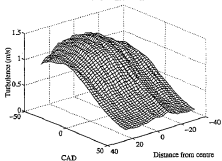*Fig. 23: Vertical velocity for asymmetric late inlet valve closing, 8.43 mm lift.*



*Fig. 21: Turbulence for late inlet valve closing, 2x9 mm lift.*



*Fig. 24: Turbulence for asymmetric late inlet valve closing, 8.43 mm lift.*

*Fig. 25: Horizontal velocity for asymmetric late inlet valve closing, 3.6 mm lift.*
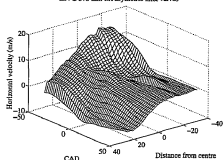


*Fig. 28: Horizontal velocity for asymmetric late inlet valve closing, 6 and 3 mm lift.*
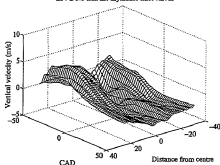


*Fig. 26: Vertical velocity for asymmetric late inlet valve closing, 3.6 mm lift.*



*Fig. 29: Vertical velocity for asymmetric late inlet valve closing, 6 and 3 mm lift.*



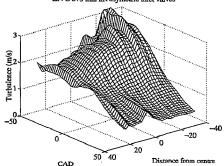*Fig. 27: Turbulence for asymmetric late inlet valve closing, 3.6 mm lift.*



*Fig. 30: Turbulence for asymmetric late inlet valve closing, 6 and 3 mm lift.*

191

*Fig. 31: Turbulence in the vicinity of the spark plug for different valve strategies.*
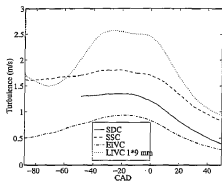


*Fig. 34: Standard deviation of turbulence in the vicinity of the spark plug for different valve strategies.*



*Fig. 32: Turbulence in the vicinity of the spark plug for different valve strategies*
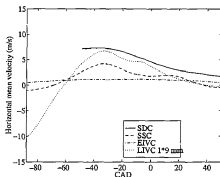


*Fig. 35: Horizontal mean velocity in the vicinity of the spark plug for different valve strategies.*



*Fig. 33: Standard deviation of turbulence in the vicinity of the spark plug for different valve strategies.*
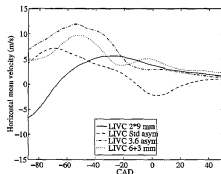


*Fig. 36: Horizontal mean velocity in the vicinity of the spark plug for different valve strategies.*
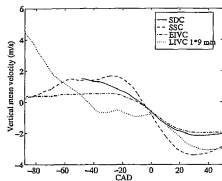
Fig. 37: Vertical mean velocity in the vicinity of the spark plug for different valve strategies.



Fig. 40: Standard deviation of mean velocity in the vicinity of the spark plug for different valve strategies.



Fig. 38: Vertical mean velocity in the vicinity of the spark plug for different valve strategies.
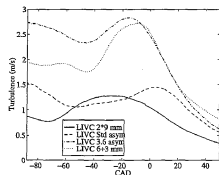


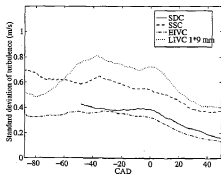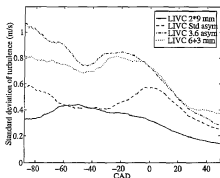Fig. 41: Anisotropy of turbulence in the vicinity of the spark plug for different valve strategies.



Fig. 39: Standard deviation of mean velocity in the vicinity of the spark plug for different valve strategies.



Fig. 42: Anisotropy of turbulence in the vicinity of the spark plug for different valve strategies.
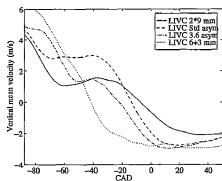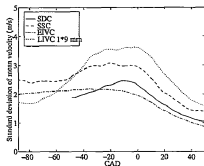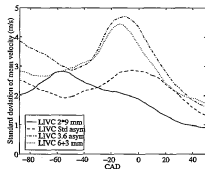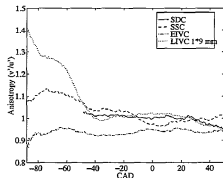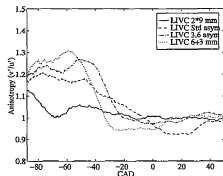
# PRESSURE MEASUREMENT RESULTS

The pressure versus crank angle data was run through a one-zone heat release model. This provides information on combustion rate and indicated mean effective pressure for the different strategies. Hereby the indicated efficiency can be calculated. The flame development period (0-10% heat release) will be presented and then main combustion (10-90% heat release). An additional look will be taken on late combustion (50-90% heat release). Some valve strategies were not run with gasoline.

GAS EXCHANGE - The gas exchange can be seen in p-V-diagrams in Figures 43-50. The pumping losses are reduced with EIVC, LIVC and with lean burn.

EFFICIENCY - The net indicated efficiency with natural gas can be seen in Fig. 51. The first two bars show the standard double cam run at $\lambda = 1.0$ and at $\lambda = 1.5$ and it can be seen that the efficiency increases with lean burn. The next two bars show the standard single cam run at $\lambda = 1.0$ and at $\lambda = 1.5$ and again, the efficiency increases with lean burn. The following five bars show the efficiency for the unthrottled cases and they all have higher efficiency than the throttled standard double cam and $\lambda = 1.0$. LIVC with 2x9 mm lift is slighly higher than the others. The highest efficiency was achieved with the standard double cam and $\lambda = 1.5$.

The gross indicated efficiency with natural gas can be seen in Fig. 52. Again it can be seen that lean burn increases the efficiency (the first four bars). The following five bars has only slightly higher efficiency gross than not due to less throttling. The last three bars, showing LIVC with asymmetric valve lift, have lower efficiency than the standard double cam run at $\lambda = 1.0$.

Figure 53 shows the net indicated efficiency with gasoline. The first four bars show that the efficiency increases with lean burn, though not very much for the standard single cam. The following four bars show the efficiency for the unthrottled valve strategies. They all have a higher efficiency than the standard double cam running at $\lambda = 1.0$. Again, LIVC with 2x9 mm lift was the best of the unthrottled strategies. Figure 54 shows the gross indicated efficiency with gasoline. The first four bars show that the throttled cases. It can be seen that lean burn increases the efficiency. The two last bars have lower gross efficiency than the standard double cam running at $\lambda = 1.0$.

FLAME DEVELOPMENT PERIOD - The flame development period is the time it takes for the flame to burn 10% of the total amount of fuel.

Natural gas- The flame development period (0-10% burned) is shown in Fig. 55. The shortest flame development period is given with an asymmetrical valve strategy and 3.6 mm lift. Very short flame development period is also given with LIVC and asymmetric valve strategy, 6+3 mm lift and LIVC, 1x9 mm lift. Standard single cam also gives a shorter flame development period than the standard double cam. All the other valve strategies are slower than the standard case and the longest flame development period is given with late inlet valve closing, 9 mm lift.

Gasoline - The flame development period for gasoline can be seen in Fig. 56. The standard single cam and the asymmetric valve strategy with 3.6 mm lift had a shorter flame development period than the standard double cam. All the other strategies had longer flame development period and the longest flame development period was given with LIVC, 2x9 mm lift.

COMBUSTION DURATION - The time it takes the engine to burn 10-90% of the total air/fuel mixture is called the main combustion.

Natural gas - The combustion duration (10-90% burnt) can be seen in Fig. 57. The fastest combustion is given with an asymmetric valve strategy and 3.6 mm lift. Standard single cam, late inlet valve closing and deactivation and asymmetric valve strategy with 6+3 mm lift had all slightly slower combustion, but they were all faster than the standard double cam. Early inlet valve closing was also slightly faster than the standard double cam, but all the other strategies gave a slower combustion. The slowest combustion was given with an asymmetric valve strategy and 8.43 mm lift. This was probably due to unfavorable horizontal mean velocity, increasing wall cooling of the flame.

Gasoline - The combustion duration for gasoline can be seen in Fig. 58. The standard single cam, $\lambda = 1.0$, early inlet valve closing and asymmetric valve strategy with 3.6 mm lift was faster than the standard double cam, $\lambda = 1.0$. All the other strategies were slower and the slowest combustion was given with the standard double cam with lean burn ($\lambda = 1.5$).

LATE COMBUSTION - The time it takes the engine to burn 50-90% of the total air/fuel mixture is called the late combustion. This is added to see if the combustion rate is constant.

Natural gas - The late combustion shows the same trend as the combustion duration. However, LIVC with 2x9 mm lift is relatively faster in the late combustion.

Gasoline - Late inlet valve closing with 2x9 mm lift is relatively faster in the late combustion.

COV IMEP - The coefficient of variance (COV) of IMEP is used as a measure of the combustion stability.

Natural gas - It can be seen in Fig. 56 that the combustion is less stable (high COV IMEP) when the engine is operating lean. Early inlet valve closing and LIVC with high lift (2x9 mm and asym. 8.43 mm) also gives high COV IMEP.

Gasoline - In Fig. 57, the COV IMEP is plotted for gasoline, and it can be seen that gasoline renders more stable combustion (low COV IMEP). Low lift also gives stable combustion (EIVC and LIVC asym. 3.6 mm).

PMEP - In Figs. 58-59 the pumping mean effective pressure can be seen for the different valve strategies. Early inlet valve closing and the throttled cases have large PMEP.
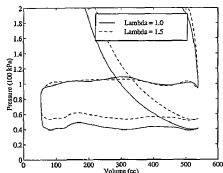
Fig. 43: Gas exchange for the standard double cam, $\lambda = 1.0$ (reference) and $\lambda = 1.5$. As can be seen the pumping losses are reduced with lean burn (the enclosed area is smaller)



Fig. 46: Gas exchange for late inlet valve closing and 1x9 mm lift. The pumping losses are reduced (the enclosed area is smaller) compared to the reference.
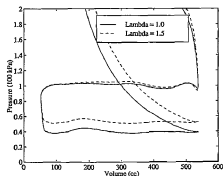


Fig. 44: Gas exchange for the standard single cam, $\lambda = 1.0$ and $\lambda = 1.5$. As can be seen the pumping losses are reduced with lean burn (the enclosed area is smaller)
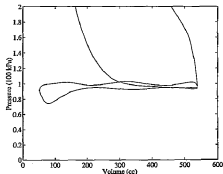


Fig. 47: Gas exchange for late inlet valve closing with 2x9 mm lift. The enclosed area represents the pumping losses and they are small compared to the reference.
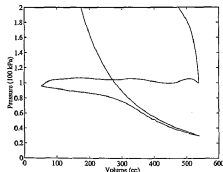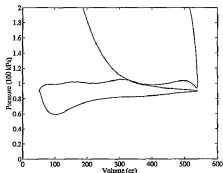


Fig. 45: Gas exchange for early inlet valve closing. The pumping losses, represented by the enclosed area, are reduced compared to the reference.



Fig. 48: Gas exchange for late inlet valve closing with an asymmetric 8.43 mm lift. The pumping losses are greatly reduced compared to the reference (smaller enclosed area).

195
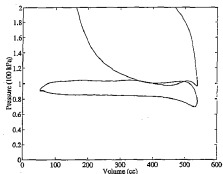
*Fig. 49: Gas exchange for late inlet valve closing with an asymmetrical 3.6 mm lift. The pumping losses are greatly reduced, compared to the reference.*
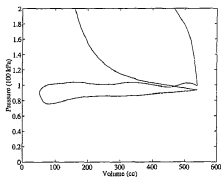


*Fig. 50: Gas exchange for late inlet valve closing with an asymmetrical 6 and 3 mm lift. The pumping losses are greatly reduced compared to the reference.*
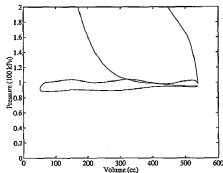


*Fig. 51: Net indicated efficiency for the different valve strategies with natural gas.*
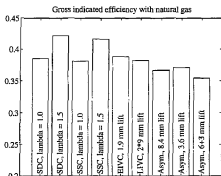


*Fig. 52: Gross indicated efficiency for the different valve strategies with natural gas.*



*Fig. 53: Net indicated efficiency for the different valve strategies with gasoline.*
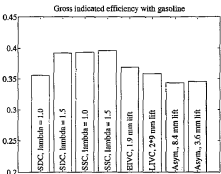


*Fig. 54: Gross indicated efficiency for the different valve strategies with gasoline.*
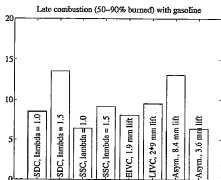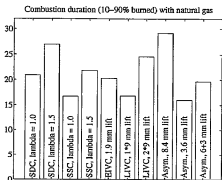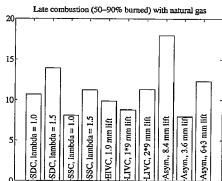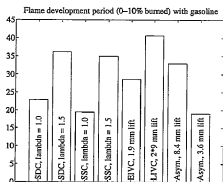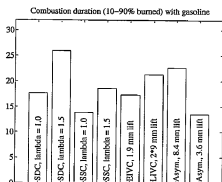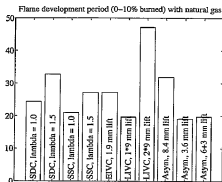
Fig. 55: Flame development period (0–10% burned) for the different valve strategies with natural gas.



Fig. 56: Flame development period (0-10% burned) for the different valve strategies with gasoline.



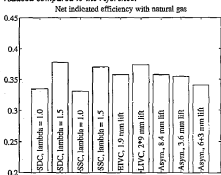Fig. 57: Combustion duration (10-90% burned) for the different valve strategies with natural gas.



Fig. 58: Combustion duration (10-90% burned) for the different valve strategies with gasoline.



Fig. 59: Late combustion (50-90% burned) for the different valve strategies with natural gas.



Fig. 60: Late combustion (50-90% burned) for the different valve strategies with gasoline.

197
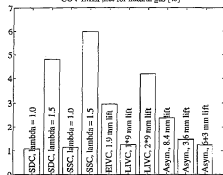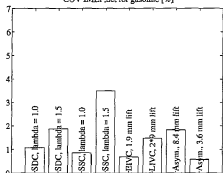
Fig. 61: COV IMEP for the different valve strategies with natural gas.
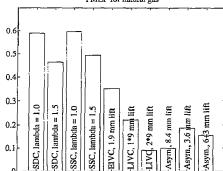


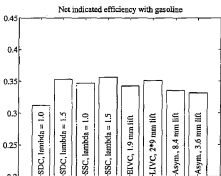Fig. 63: PMEP for the different valve strategies with natural gas.



Fig. 62: COV IMEP for the different valve strategies with gasoline.
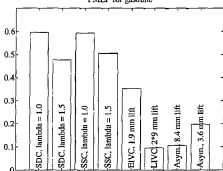


Fig. 64: Pumping mean effective pressure for the different valve strategies with gasoline.

## DISCUSSION

STANDARD VALVE CLOSING - With the standard cam-shaft and throttling (the reference strategy), the pressure is lowered during the induction stroke. Low pressure cools the inlet charge and vaporization is impaired. Some increase in heat transfer from the cylinder walls might improve vaporization. The major drawback is the great pumping loss during part load.

Standard valve closing with throttling gives a tumbling flow with an increase in turbulence at TDC due to tumble breakdown. The combustion is slow and this is why inlet valve deactivation often is used at part load and at low speeds. This increases the turbulence by creating swirl and the combustion gets faster and more stable. However, the indicated efficiency is lower with inlet valve deactivation. This is probably due to greater heat losses during the combustion and expansion phase.

One way of increasing the efficiency is lean burn. Lean burn reduces the pumping losses and it also increases the ratio of specific heat during compression and expansion.. The combustion gets more unstable with lean burn, but this can be improved with the generation of higher turbulence, e.g. by using valve deactivation.

EARLY INLET VALVE CLOSING - The open duration of the valve, with early inlet valve closing, is very short. This also influences the valve lift; it can only be 1.9 mm. Otherwise, the contact stresses on the valves are too large. The early valve closing also means relatively long time for the flow to slow down, reducing mean velocity and turbulence at the time of ignition.

Pumping mean effective pressure is high for EIVC. This is partly due to valve throttling, created by the low lift, and partly due to the PMEP definition. The pumping loss is not large.

The volume increases and the pressure decreases, during the induction, which cools the inlet charge. This can make the heat transfer across the cylinder walls greater and the charge hotter after compression. This improves the vaporization of the fuel droplets when the engine is running on gasoline and this makes the combustion more stable. This is indicated by the low COV_IMEP which can be seen in Fig. 62.

One drawback of early inlet valve timing, is that it gives some pumping losses due to the low lift of the valves. This may be improved by electro-hydraulic valve control, which enables faster valve lifts, at least for low speeds.

LATE INLET VALVE CLOSING - With late inlet valve closing, the pumping losses are greatly reduced. This increases the overall efficiency of the engine if the combustion does not deteriorate. However, with late inlet valve closing, there is much charge heating from the cylinder walls, and this might affect combustion stability, see Figs. 61-62.

Late inlet valve closing with an asymmetric 8.43 mm lift gave higher turbulence than the standard double cam, but the standard double cam had a shorter flame development period and a faster combustion duration. This is probably due to the high vertical velocity for the LIVC case during the flame development period. The high vertical velocity pushes the flame up against the cylinder head with large flame cooling as a possible result.

Late inlet valve closing, 2x9 mm lift has more turbulence than EIVC but a longer flame development. This might be due to vertical and horizontal velocity pushing the flame up against the spark plug. This cooling effect might explain the very long flame development. The late combustion, however, is almost as fast as it is for EIVC, as can be seen in Figs. 59 and 60.

## CONCLUSIONS

- Early inlet valve closing gave low horizontal and vertical mean velocity in the cylinder. The turbulence intensity is also reduced.

- Early inlet valve closing gave stable combustion with gasoline. This is probably due to additional charge heating during induction and compression. It might also be the low lift that creates a shearing air flow. This flow atomizes the fuel droplets and gives better fuel/air mixture.

- Late inlet valve closing with an asymmetric 3.6 mm lift gave the most stable combustion for gasoline fueling. This is probably due to high turbulence and favorable mean velocity, minimizing wall cooling.

- Lean burn increases the efficiency relatively much. This is due to less throttling and higher gamma (i.e. the ratio of specific heat) during compression and expansion.

- Gross indicated efficiency is reduced with strategies giving high turbulence. This is probably due to the high turbulence intensity, which increases heat losses.

- Pumping mean effective pressure is greatly reduced for the unthrottled cases, except for early inlet valve closing. This is due to the PMEP definition. The pumping loss for EIVC, compared to the throttled case, is, however, greatly reduced.

- Pumping mean effective pressure is higher for the strategies giving high turbulence.

## REFERENCES

[1]  M. M. Schechter, M. B. Levin; "Camless engine", SAE paper 960581.

[2]  M. A. Theobald, B. Lequesne, R. Henry, GM; "Control of Engine Load via Electromagnetic Valve Actuation". SAE paper 940816.

[3]  T. Dresner, P. Barkan; "A Review and Classification of Variable Valve Timing Mechanisms", SAE paper 890674.

[4]  N. D. Wilson, A. J. Watkins, C. Dopson; "Asymmetric Valve Strategies and Their Effect on Combustion", SAE paper 930821

[5]  B. Johansson, F. Söderberg; "The Effect of Valve Strategy on In-Cylinder Flow and Combustion", SAE paper 960582.

[6]   F.E. Corcione, G. Valentino; "Cycle-resolved LDV measurements in an IC Engine Equipped with Different Combustion Chamber Shapes", Applications of Laser Anemometry to Fluid Mechanics, 4th Int. Symp. Lisbon, Portugal, 1988

[7]   G. Woschni; "A Universally Applicable Equation for Instantaneous Heat Transfer Coefficient in the Internal Combustion Engine", SAE670931.

[8]   B. Johansson; "Correlation Between Velocity Parameters Measured with Cycle-Resolved 2-D LDV and Early Combustion in a Spark Ignition Engine", Licentiate Thesis, ISRN LUTMDN/TMVK7012SE, Dept. of Heat & Power Engineering, Lund Institute of Technology, 1993

## ABBREVIATIONS

| | | |
|---|---|---|
| ABDC | = | after BDC |
| asym. | = | asymmetric, asymmetrical |
| ATDC | = | after TDC |
| BBDC | = | before BDC |
| BDC | = | bottom dead center |
| BMEP | = | brake mean effective pressure |
| BTDC | = | before TDC |
| CAD | = | crank angle degree |
| COV | = | coefficient of variance |
| EGR | = | exhaust gas recirculation |
| EIVC | = | early inlet valve closing |
| IMEP | = | indicated mean effective pressure |
| $\lambda$ | = | lambda, air/fuel ratio. $\lambda = 1.0$ is stoichiometry. |
| LIVC | = | late inlet valve closing |
| LDV | = | laser doppler velocimetry |
| MBT | = | maximum brake torque |
| PMEP | = | pumping mean effective pressure |
| SDC | = | standard double cam, represents the reference cam shaft. |
| SSC | = | standard single cam, represents the reference cam shaft with valve deactivation. |
| TDC | = | top dead center |